The 5th Joint International Conference on Multibody System Dynamics
June 24 – 28, 2018, Lisboa, Portugal

A system-level bushing joint parameter identification approach using flexible multibody models

Simon Vanpaemel[1,2], Martijn Vermaut[1,2], Frank Naets[1,2] and Wim Desmet[1,2]

[1]*PMA, KU Leuven, {simon.vanpaemel, martijn.vermaut, frank.naets, wim.desmet}@kuleuven.be*
[2]*DMMS Lab, Flanders Make*

ABSTRACT — *In this work, the authors propose a technique for identifying bushing parameters in-situ using system-level measurements and (flexible) multibody models. The sensitivity information employed for the optimization, is obtained using the Adjoint Variable Method (AVM). This method has the advantage of obtaining sensitivity information at a computational cost independent of the amount of design parameters. The proposed approach has been implemented in an in-house object-oriented Matlab multibody code. The underlying flexible multibody formulation employed is a novel approach called the flexible natural coordinate formulation (FNCF). This formulation combines the properties of the floating frame of reference (FFR) and the generalized component mode synthesis (GCMS) method and results in a constant mass and stiffness matrix with quadratic constraint equations. The specific equation structure obtained through the FNCF formulation drastically reduces the complexity of the AVM as the simulation derivatives can be readily obtained and are of limited order. The procedure for bushing parameter identification is illustrated by the identification of a bushing modeled by the Kelvin-Voigt model.*

---

1 Introduction

Bushings are a key component in the proper operation of mechanical systems, ranging from vehicles to production machinery. These bushings have a high impact on the dynamic loads and vibrations transferred through the system. Due to their high importance, an accurate characterization of these components is key in the design and monitoring of these mechanical systems. However, in current practice this characterization for operationally representative boundary conditions and load cases is lacking. Experimental parameter identification methods exist, but these are typically limited to isolated identification on dedicated test rigs [1, 2, 3]. On the other hand, a fully (nonlinear) finite-element model is typically not available either.

In this work, we propose a technique for identifying bushing parameters in-situ using system-level measurements and (flexible) multibody models. These models can contain of a large amount of bushings, each represented with a specific bushing model and the associated parameters. This identification is performed by minimizing the difference between the measured and simulated response of the multibody system. However, for a large number of bushing parameters and large multibody models this optimization can become very computationally demanding.

Often optimizers employ sensitivity information in order to obtain faster convergence [4]. However, the generation of this information comes at a cost, which depends on the employed sensitivity method. There exist a variety of methods, of which finite differences, direct differentiation [5, 6], the adjoint variable method (AVM) [6, 7] and automatic differentiation [8] are most notable. The efficiency and accuracy of these methods with respect to each other, depend heavily on the specific optimiation problem.

Finite differences is a numerical method which is very easy to implement as an add-on to existing multibody software, but has a relatively low accuracy due to perturbation errors. Moreover the computational complexity scales with the amount of design parameters, which rapidly becomes unacceptable.

The direct differentiation method is a symbolic method which is stable and numerically exact. This method differentiates the equations of motion with respect to the design parameters, and solves this system for the derivatives of the state variables.
The automatic differentiation method is based on systematically applying the differentiation chain rule to computer programs. It is as accurate as an analytical method, and much easier to implement since it can be done automatically. Automatic differentiation algorithms compute the derivatives of the state variables alongside the normal integration of the equation of motion. However, this process can be computationally costly if an implicit time-integrator converges to high precision, since the code computes the sensitivities at each iteration [9]. Although this method systematically applies the differentiation chain rule, it cannot be classified as a symbolic method since the evaluations of the derivatives is done numerically [10].
The AVM is a symbolic method. The authors propose to exploit this method for obtaining the sensitivity information for bushing parameters in flexible multibody models. This method has the advantage that as the computational complexity does not scale with the amount of design parameters, it is very well suited for problems with a lot of design parameters. Key in this method is to compute adjoint variables which are used to obtain the sensitivity information. The computation of the adjoint variables takes equal or less time than the forward integration of the equations of motion [11]. The drawback is that the method results in more complex equations to be solved and a large data storage of variables for the backward integration. [10]
The adjoint variables are obtained by a backward integration in time of the adjoint system, which is described by differential algebraic equations (DAE). The equations are based on the variation of the functional and the equations of motion (EOM). The use of a (flexible) multibody formulation of which these variations drop out, or are of low complexity, reduces the computational cost of the sensitivity information. In this work we therefore propose to exploit the flexible natural coordinate formulation (FNCF) recently introduced by Vermaut *et al.* [12]. The specific equation structure obtained through the FNCF formulation drastically reduces the complexity of the AVM as the simulation derivatives can be readily obtained and are of limited order.
In this work, first an overview of the parameter identification process is discussed in section 2. Section 3 gives a brief summary of the FNCF flexible multibody formulation. Section 4 focuses on the application of the FNCF formulation on the AVM. Finally, sections 5 and 6 respectively discuss the results and the conclusions of this work.

2 Parameter identification framework

A flowchart of the parameter identification process is shown in Figure 1. The process starts with an initial guess of the design parameters $\boldsymbol{\rho}_{init} \in \mathbb{R}^{n_\rho}$, followed by the computation of the residual of the objective function ψ and its sensitivity information $\nabla_{\boldsymbol{\rho}}\psi \in \mathbb{R}^{n_\rho}$. If the residual is above an user specified threshold, a new iteration starts with a new guess $\boldsymbol{\rho}^* \in \mathbb{R}^{n_\rho}$ of the design parameters. If the optimizer converges to a local minimum, it will output the converged parameter values $\boldsymbol{\rho}_{end} \in \mathbb{R}^{n_\rho}$.

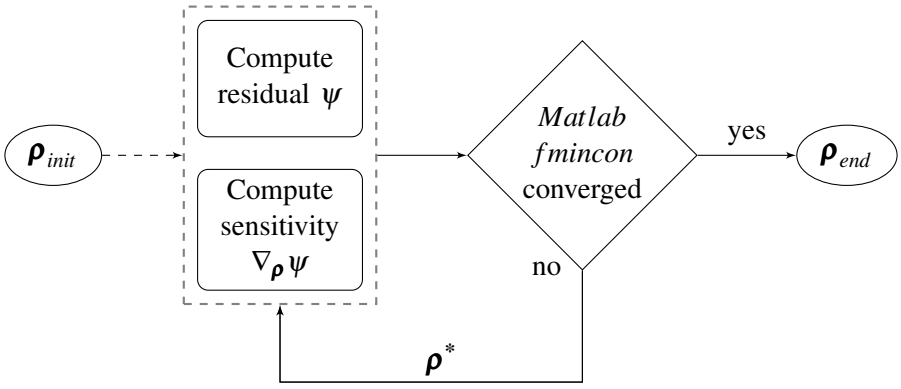

Fig. 1: Process of parameter identification

In general the objective function ψ, is a time integration with starting time T_0 and ending time T_F of the least

squares error between time signals, g, in combination with some end-point constraints w:

$$\psi = w(\mathbf{q}_F, \dot{\mathbf{q}}_F, \ddot{\mathbf{q}}_F, \boldsymbol{\rho}_F, \boldsymbol{\lambda}_F) + \int_{T_0}^{T_F} g(\mathbf{q}, \dot{\mathbf{q}}, \ddot{\mathbf{q}}, \boldsymbol{\lambda}, \boldsymbol{\rho})\, \mathrm{d}t \tag{1a}$$

$$g = (y(\mathbf{q}, \dot{\mathbf{q}}, \ddot{\mathbf{q}}, \boldsymbol{\lambda}, \boldsymbol{\rho}) - \hat{y}(t))^2 \tag{1b}$$

The least squares error is computed between a simulated signal y and a measured signal $\hat{y}$. The signals can be positions, velocities, accelerations, forces, etc... which in general depend on the generalized coordinates $\mathbf{q} = \begin{bmatrix} \mathrm{q}_1 & \mathrm{q}_2 & \cdots & \mathrm{q}_{\mathrm{n_q}} \end{bmatrix} \in \mathbb{R}^{n_q}$, velocities $\dot{\mathbf{q}} \in \mathbb{R}^{n_q}$, accelerations $\ddot{\mathbf{q}} \in \mathbb{R}^{n_q}$, Lagrangian multipliers $\boldsymbol{\lambda} \in \mathbb{R}^{n_\lambda}$ and the design parameters $\boldsymbol{\rho} \in \mathbb{R}^{n_\rho}$. The simulated signal is in this work obtained using the FNCF (small deformation) flexible multibody formulation.
The subscript $()_0$ denotes the evaluation at time T_0, the subscript $()_F$ denotes the evaluation of the variables at time T_F, The superscript $\dot{()}$ denotes time derivative of that specific variable.

The focus in this work lies on the computation of the sensitivity information, this is discussed in section 4. First a brief overview of the underlying FNCF multibody formulation is given in section 3.

3 Flexible Natural Coordinate Formulation

FNCF is a small deformation flexible multibody formulation that results in constant mass and stiffness matrices with quadratic constraint equations. Moreover no quadratic velocity term appears, as is the case when using a Floating Frame of Reference (FFR) multibody formulation, nor a term which is nonlinear in the flexible deformation, as is the case when using a Generalized Component Mode Synthesis (GCMS) multibody formulation. This specific equation structure obtained through the FNCF formulation drastically reduces the complexity of the AVM as the simulation derivatives can be readily obtained and are of limited order. The cost of obtaining this equation structure is the introduction of redundancy in the set of generalized coordinates. The majority of the equations in this section are discussed in detail in [12].

The generalized coordinate vector $\mathbf{q}$ used in sections 3.1 and 3.2 contains only the generalized coordinates associated with a single flexible body, as indicated in Equation (2). The assembled system is only considered from section 3.3 onwards.

3.1 Kinematics of a single body

The generalized coordinates $\mathbf{q}$ of a flexible body using the FNCF formulation, can be denoted as

$$\mathbf{q} = \begin{bmatrix} \boldsymbol{\sigma} \\ \boldsymbol{\pi} \\ \boldsymbol{\gamma} \\ \boldsymbol{\delta} \end{bmatrix} \tag{2}$$

which consists of 4 'types' of coordinates. First, $\boldsymbol{\sigma} \in \mathbb{R}^3$ which defines the position of the reference frame of the body. Second, $\boldsymbol{\pi} \in \mathbb{R}^9$ are redundant coordinates that parametrize the rotation matrix of the body. Third, $\boldsymbol{\delta} \in \mathbb{R}^{n_\delta}$ are the participation factors of the modes $\boldsymbol{\Psi} \in \mathbb{R}^{\mathrm{N} \times n_\delta}$ used to reduce the FE model , with n_δ the amount of modes. These participation factors describe the deformation in the body-fixed reference frame, as in the FFR multibody formulation. Fourth, The FNCF introduces new, but redundant, coordinates $\boldsymbol{\gamma} \in \mathbb{R}^{9 n_\delta}$, computed from $\boldsymbol{\pi}$ and $\boldsymbol{\delta}$ using a Kronecker product:

$$\boldsymbol{\gamma} = \boldsymbol{\delta} \otimes \boldsymbol{\pi} \tag{3}$$

These coordinates enable a linear relationship between the generalized coordinates $\mathbf{q}$ and the position $\mathbf{u}^{(p)}$ of a point p on a deformable body, using a constant projection matrix $\mathbf{r}_{\mathbf{q}}^{(p)} \in \mathbb{R}^{3 \times (12 + 10 n_\delta)}$:

$$\mathbf{u}^{(p)} = \begin{bmatrix}\mathbf{I}_3 & \mathbf{r}_{\boldsymbol{\pi}}^{(p)} & \mathbf{r}_{\boldsymbol{\gamma}}^{(p)} & \mathbf{0}_{3\times \mathrm{n}_\delta}\end{bmatrix}\begin{bmatrix}\boldsymbol{\sigma}\\ \boldsymbol{\pi}\\ \boldsymbol{\gamma}\\ \boldsymbol{\delta}\end{bmatrix} = \mathbf{r}_{\mathbf{q}}^{(p)}\mathbf{q} \quad \Rightarrow \quad \begin{cases}\dot{\mathbf{u}}^{(p)} = \mathbf{r}_{\mathbf{q}}^{(p)}\dot{\mathbf{q}}\\ \ddot{\mathbf{u}}^{(p)} = \mathbf{r}_{\mathbf{q}}^{(p)}\ddot{\mathbf{q}}\end{cases} \tag{4}$$

The rotation matrix of a point p, describing rigid body rotation and the rotation due to the small deformation, can be written as follows:

$$\mathbf{R}^{(p)} = \sum_{i=1}^{9}\mathbf{P}_i\pi_i + \sum_{i=1}^{9n_\delta}\mathbf{R}_{\gamma,i}^{(p)}\gamma_i \tag{5}$$

wherein $\mathbf{P}_i \in \mathbb{R}^{3\times3}$ and $\mathbf{R}_{\gamma,i}^{(p)} \in \mathbb{R}^{3\times3}$ are both constant shape matrices. This results in a rotation matrix being linear in the generalized coordinates $\mathbf{q}$. This is not the case using another multibody formulation such as FFR or GCMS, of which the rotation matrix is nonlinear in the generalized coordinates.

3.2 Dynamics of a single body

The deformations of the flexible bodies are assumed small, such that the linear finite element (FE) mass and stiffness matrices, $\mathbf{M}^{\mathrm{FE}} \in \mathbb{R}^{\mathrm{N}\times\mathrm{N}}$ and $\mathbf{K}^{\mathrm{FE}} \in \mathbb{R}^{\mathrm{N}\times\mathrm{N}}$ respectively, are constant. It is assumed that $\mathbf{M}^{\mathrm{FE}}$ is a lumped mass matrix. The FE mass matrix can be reduced to the reduced generalized mass matrix $\mathbf{M}_{\mathbf{qq}}$ using the constant projection matrix $\mathbf{r}_{\mathbf{q}}$:

$$\mathbf{M}_{\mathbf{qq}} = \mathbf{r}_{\mathbf{q}}^{\mathrm{T}}\mathbf{M}^{\mathrm{FE}}\mathbf{r}_{\mathbf{q}} \tag{6}$$

This projection matrix is a generalization of the projection matrix $\mathbf{r}_{\mathbf{q}}^{(p)}$, for all nodes in the FE model. Note that the reduced mass matrix is constant and thus independent of the generalized coordinates $\mathbf{q}$. Because the projection matrix $\mathbf{r}_{\mathbf{q}}$ is nonlinear in the case of the FFR multibody formulation, it ends up with a nonlinear reduced mass matrix.

The computation of the reduced stiffness matrix $\mathbf{K}_{\mathbf{qq}}$ is equivalent to the FFR multibody formulation:

$$\mathbf{K}_{\mathbf{qq}} = \begin{bmatrix}\mathbf{0}_{(12+9n_\delta)\times\mathrm{N}}\\ \boldsymbol{\Psi}^{\mathrm{T}}\end{bmatrix}\mathbf{K}^{\mathrm{FE}}\begin{bmatrix}\mathbf{0}_{\mathrm{N}\times(12+9n_\delta)} & \boldsymbol{\Psi}\end{bmatrix}. \tag{7}$$

This is the reason that the coordinates $\boldsymbol{\delta}$ are still included in the generalized coordinate vector $\mathbf{q}$ besides $\boldsymbol{\gamma}$, as the resulting reduced stiffness matrix is constant and thus independent of the generalized coordinates $\mathbf{q}$. The GCMS formulation on the other hand ends up with a non-linear reduced stiffness matrix, since these local coordinates are not included generalized coordinate vector.

3.3 FNCF constraints

The constraint equations of a (flexible) multibody systems can be divided into two groups. The first group are constraints which apply to a single (flexible) body, e.g. the orthonormality constraints of the body's rotation matrix and the introduction of the redundant coordinates $\boldsymbol{\gamma}$, given by equation (3), which are both quadratic in the generalized coordinates. The second group are constraints that are applied between different (flexible) components. These constraints are often called joint constraints and are assumed to be holonomic in this work. They enable the modeling of ideal spherical, translational, revolute, etc... joints. These constraints are linear or quadratic in the generalized coordinates as well.
Since the complete set of constraint equations are at most quadratic in the generalized coordinates, it is possible to write the constraint equations as a Taylor expansion around $\mathbf{q} = \mathbf{0}$:

$$\boldsymbol{\phi} = C_0 + \mathbf{J}_0\mathbf{q} + \frac{1}{2}\left(\sum_i \mathbf{H}_{0,i}\mathbf{q}_i\right)\mathbf{q} = \mathbf{0} \tag{8}$$

wherein $\mathbf{J}_0$ and $\mathbf{H}_{0,i}$ are constant matrices.

3.4 Equations of motion

The reduced mass $\mathbf{M_{qq}}$ and stiffness matrices $\mathbf{K_{qq}}$ of the flexible bodies can now be assembled in the mass and stiffness matrices of the complete multibody system, denoted as $\mathbf{M}$ and $\mathbf{K}$ respectively.
The fully assembled equations of motion can be summarized as:

$$\begin{cases} \mathbf{M}\ddot{\mathbf{q}} + \frac{\partial \boldsymbol{\phi}}{\partial \mathbf{q}}^{\mathrm{T}}\boldsymbol{\lambda} = \mathbf{f} \\ \boldsymbol{\phi} = \mathbf{0} \end{cases} \tag{9}$$

with:

$$\mathbf{f} = \mathbf{f}_{gra} - \mathbf{C}\dot{\mathbf{q}} - \mathbf{K}\mathbf{q} + \mathbf{f}_{ext} + \mathbf{f}_{bus} \tag{10}$$

where $\mathbf{f}_{ext}$ is the generalized force vector of the externally applied loads, $\mathbf{f}_{bus}$ is the generalized force vector of the bushing loads acting between the components. The reduced damping matrix is denoted as $\mathbf{C}$, which is constant for viscous damping on the deformations. The generalized force vector $\mathbf{f}_{gra}$ of the gravity force is constant because of the constant projection matrix $\mathbf{r_q}$, it can be written as follows: $\mathbf{f}_{gra} = \mathbf{r}_{\mathbf{q}}^{\mathrm{T}}\mathbf{M}^{\mathrm{FE}}\mathbf{g}$.
Note that the projection matrices between the external loads applied in a local or global frame $\boldsymbol{\upsilon}_{ext}$ and the generalized external force vector $\mathbf{f}_{ext}$ are constant or linear in the generalized coordinates. This is not the case when using either a FFR or GCMS multibody formulation, since these end up with complex non-linear projection matrices.

4 FNCF applied to AVM

The FNCF formulation and its advantageous properties are immediately applied to the equations of the adjoint system which are obtained from [13]. Moreover, several assumptions are assumed in this work:

- No end-point constraints: $w = 0$.
- The system is initially at rest: $\left(\frac{\partial \dot{\mathbf{q}}}{\partial \boldsymbol{\rho}}\right)_{T_0} = 0$.
- The design parameters $\boldsymbol{\rho}$ are bushing parameters, thus only appearing in the generalized force term $\mathbf{f}_{bus}$. This leads to the elimination of $\frac{\partial^2 \boldsymbol{\phi}}{\partial \mathbf{q}\partial \boldsymbol{\rho}}$, $\frac{\partial \mathbf{M}}{\partial \boldsymbol{\rho}}$ and $\frac{\partial \boldsymbol{\phi}}{\partial \boldsymbol{\rho}}$.

the resulting adjoint system reduces to the following set of equations:

$$\begin{cases} \mathbf{M}^{\mathrm{T}}\ddot{\boldsymbol{\mu}} + \frac{\partial \mathbf{f}}{\partial \dot{\mathbf{q}}}^{\mathrm{T}}\dot{\boldsymbol{\mu}} + \left(\frac{\partial^2 \boldsymbol{\phi}}{\partial \mathbf{q}\partial \mathbf{q}}^{\mathrm{T}} \otimes \lambda - \frac{\partial \mathbf{f}}{\partial \mathbf{q}} + \frac{\mathrm{d}}{\mathrm{dt}}\left(\frac{\partial \mathbf{f}}{\partial \dot{\mathbf{q}}}\right)\right)^{\mathrm{T}}\boldsymbol{\mu} + \frac{\partial \boldsymbol{\phi}}{\partial \mathbf{q}}^{\mathrm{T}}\boldsymbol{\mu}_{\boldsymbol{\phi}} = \frac{\partial \mathrm{g}}{\partial \mathbf{q}}^{\mathrm{T}} - \frac{\mathrm{d}}{\mathrm{dt}}\left(\frac{\partial \mathrm{g}}{\partial \dot{\mathbf{q}}}^{\mathrm{T}}\right) + \frac{\mathrm{d}^2}{\mathrm{dt}^2}\left(\frac{\partial \mathrm{g}}{\partial \ddot{\mathbf{q}}}^{\mathrm{T}}\right) \\ \frac{\partial \boldsymbol{\phi}}{\partial \mathbf{q}}\boldsymbol{\mu} = \frac{\partial \mathrm{g}}{\partial \boldsymbol{\lambda}}^{\mathrm{T}} \end{cases} \tag{11}$$

This system must be solved backward in time, by using following 'initial' conditions at time T_F :

$$\left[\mathbf{M}^{\mathrm{T}}\dot{\boldsymbol{\mu}}+\frac{\partial \mathbf{f}}{\partial \dot{\mathbf{q}}}^{\mathrm{T}}\boldsymbol{\mu}+\frac{\partial \boldsymbol{\phi}^{\mathrm{T}}}{\partial \mathbf{q}}\boldsymbol{\gamma}+\left(\frac{\partial^2\boldsymbol{\phi}}{\partial \mathbf{q}\partial \mathbf{q}}\otimes\dot{\mathbf{q}}+\frac{\partial^2\boldsymbol{\phi}}{\partial \mathbf{q}\partial \mathrm{t}}\right)^{\mathrm{T}}\boldsymbol{\eta}\right]_{T_F} = \left[\frac{\mathrm{d}}{\mathrm{dt}}\left(\frac{\partial \mathrm{g}}{\partial \ddot{\mathbf{q}}}^{\mathrm{T}}\right)-\left(\frac{\partial \mathrm{g}}{\partial \dot{\mathbf{q}}}^{\mathrm{T}}\right)\right]_{T_F} \tag{12a}$$

$$\left[\mathbf{M}^{\mathrm{T}}\boldsymbol{\mu}+\frac{\partial \boldsymbol{\phi}^{\mathrm{T}}}{\partial \mathbf{q}}\boldsymbol{\eta}\right]_{T_F} = \left[\frac{\partial \mathrm{g}}{\partial \ddot{\mathbf{q}}}^{\mathrm{T}}\right]_{T_F} \tag{12b}$$

$$\left[\frac{\partial \boldsymbol{\phi}}{\partial \mathbf{q}}\boldsymbol{\mu}\right]_{T_F} = \left[\frac{\partial \mathrm{g}}{\partial \boldsymbol{\lambda}}^{\mathrm{T}}\right]_{T_F} \tag{12c}$$

$$\left[\frac{\partial \boldsymbol{\phi}}{\partial \mathbf{q}}\dot{\boldsymbol{\mu}}+\frac{\partial \dot{\boldsymbol{\phi}}}{\partial \mathbf{q}}\boldsymbol{\mu}\right]_{T_F} = \left[\frac{\mathrm{d}}{\mathrm{dt}}\left(\frac{\partial \mathrm{g}}{\partial \boldsymbol{\lambda}}^{\mathrm{T}}\right)\right]_{T_F} \tag{12d}$$

The sensitivity of the objective function w.r.t. the design parameters can then be computed as follows:

$$\nabla_{\boldsymbol{\rho}}\psi^{\mathrm{T}} = \left[\left(\frac{\mathrm{d}}{\mathrm{dt}}\left(\frac{\partial \mathrm{g}}{\partial \ddot{\mathbf{q}}}\right)-\frac{\partial \mathrm{g}}{\partial \dot{\mathbf{q}}}-\dot{\boldsymbol{\mu}}^{\mathrm{T}}\mathbf{M}-\boldsymbol{\mu}^{\mathrm{T}}\frac{\partial \mathbf{f}}{\partial \dot{\mathbf{q}}}\right)\frac{\partial \mathbf{q}}{\partial \boldsymbol{\rho}}\right]_{T_0}+\int_{T_0}^{T_F}\left(\frac{\partial \mathrm{g}}{\partial \boldsymbol{\rho}}-\boldsymbol{\mu}^{\mathrm{T}}\left(-\frac{\partial \mathbf{f}}{\partial \boldsymbol{\rho}}\right)\right)\mathrm{dt} \tag{13}$$

The following sections 4.1 to 4.2 elaborate on the terms appearing in Equations 11 to 13. The focus lies on the computation of the partial derivatives when employing the underlying FNCF multibody formulation.

4.1 Derivatives of the constraint equations

Since the constraint equations (8) are quadratic in the generalized coordinates, the first order partial derivative with respect to the generalized coordinates $\mathbf{q}$ results in a linear dependence of the generalized coordinates:

$$\frac{\partial \boldsymbol{\phi}}{\partial \mathbf{q}} = \mathbf{J}_0+\left(\sum_{\mathrm{i}}\mathbf{H}_{0,\mathrm{i}}\mathbf{q}_{\mathrm{i}}\right) \tag{14}$$

Similarly, the second order partial derivatives results in a constant matrix:

$$\frac{\partial^2\boldsymbol{\phi}}{\partial \mathbf{q}_{\mathrm{i}}\partial \mathbf{q}} = \mathbf{H}_{0,\mathrm{i}} \qquad\qquad \mathrm{i} = 1, 2, \ldots, \mathrm{n_q} \tag{15}$$

4.2 Derivatives of the generalized forces

This section focuses on the derivatives of the generalized force vector $\mathbf{f}(\mathbf{q},\dot{\mathbf{q}},\boldsymbol{\rho})$, Equation (10), which depends on the design parameters via the generalized force term of the bushings $\mathbf{f}_{bus}(\mathbf{q},\dot{\mathbf{q}},\boldsymbol{\rho})$.
The following derivatives must be computed in order to obtain the sensitivity information:

$$\mathbf{f}_{\mathbf{q}} = \frac{\partial \mathbf{f}}{\partial \mathbf{q}} = -\mathbf{K}+\frac{\partial \mathbf{f}_{ext}}{\partial \mathbf{q}}+\frac{\partial \mathbf{f}_{bus}}{\partial \mathbf{q}} \tag{16a}$$

$$\mathbf{f}_{\dot{\mathbf{q}}} = \frac{\partial \mathbf{f}}{\partial \dot{\mathbf{q}}} = -\mathbf{C}+\frac{\partial \mathbf{f}_{ext}}{\partial \dot{\mathbf{q}}}+\frac{\partial \mathbf{f}_{bus}}{\partial \dot{\mathbf{q}}} \tag{16b}$$

$$\dot{\mathbf{f}}_{\dot{\mathbf{q}}} = \frac{\mathrm{d}}{\mathrm{dt}}\left(\frac{\partial \mathbf{f}_{ext}}{\partial \dot{\mathbf{q}}}+\frac{\partial \mathbf{f}_{bus}}{\partial \dot{\mathbf{q}}}\right) \tag{16c}$$

$$\mathbf{f}_{\boldsymbol{\rho}} = \frac{\partial \mathbf{f}}{\partial \boldsymbol{\rho}} = \frac{\partial \mathbf{f}_{ext}}{\partial \boldsymbol{\rho}}+\frac{\partial \mathbf{f}_{bus}}{\partial \boldsymbol{\rho}} \tag{16d}$$

As indicated in section 3.4 is the projection matrix between $\mathbf{f}_{ext}$ and $\boldsymbol{\upsilon}_{ext}$ at most linear in the generalized coordinates. Resulting in $\frac{\partial \mathbf{f}_{ext}}{\partial \mathbf{q}}$ being zero or constant in the generalized coordinates and $\frac{\partial \mathbf{f}_{ext}}{\partial \dot{\mathbf{q}}}$ being zero.
The following section 4.2.1 focuses the generalized bushing force vector $\mathbf{f}_{bus}$ and its derivatives.

4.2.1 Generalized bushing force vector and its derivatives

This section elaborates on the computation of the bushing loads, the projections to obtain the generalized bushing force vector and the accompanied partial derivatives.
A bushing is a flexible connection between two frames. Each frame has a position and orientation. The positions for frame 1 and 2 are given by $\mathbf{u}_1$ and $\mathbf{u}_2$ respectively. The orientations are given by rotation matrices $\mathbf{R}_1$ and $\mathbf{R}_2$, respectively for frame 1 and 2. Both the positions and orientations are resolved in a fixed world coordinate system.

The relative position and orientation between both frames are denoted as $\mathbf{x}_t$ and $\mathbf{x}_r$ respectively. Both are resolved in frame 1. It is assumed in this work that the relative angular orientation remains small.[a]

$$\mathbf{x}_t = \mathbf{R}_1^{\mathrm{T}} \left(\mathbf{u}_2^{(p)} - \mathbf{u}_1^{(p)} \right) \tag{17a}$$

$$\mathbf{x}_r = vect(\mathbf{R}_1^{\mathrm{T}} \mathbf{R}_2) \tag{17b}$$

The relative configuration between both frames can be denoted as $\mathbf{x} = \begin{bmatrix} \mathbf{x}_t \\ \mathbf{x}_r \end{bmatrix}$. The differential rotation vector of $\mathbf{R}_1^{\mathrm{T}} \mathbf{R}_2$ is denoted as $\mathrm{d}\mathbf{x}_\mathrm{r} = \mathrm{vect}\left(\mathrm{d}\left(\mathbf{R}_1^{\mathrm{T}} \mathbf{R}_2 \right) \mathbf{R}_2^{\mathrm{T}} \mathbf{R}_1 \right)$.

The relative velocities resolved in frame 1 are given by:

$$\mathbf{v}_t = \mathbf{R}_1^{\mathrm{T}} \left(\dot{\mathbf{u}}_2^{(p)} - \dot{\mathbf{u}}_1^{(p)} \right) \tag{18a}$$

$$\boldsymbol{\omega}_r = \mathbf{R}_1^{\mathrm{T}} \left(\boldsymbol{\omega}_2^{(p)} - \boldsymbol{\omega}_1^{(p)} \right) \tag{18b}$$

wherein $\boldsymbol{\omega}_1$ and $\boldsymbol{\omega}_2$ are respectively the angular velocities of frame 1 and 2, resolved in the fixed world coordinate system. The relative velocity vector is given by $\mathbf{v} = \begin{bmatrix} \mathbf{v}_t \\ \boldsymbol{\omega}_r \end{bmatrix}$. For ease of notation the superscript $()^{(p)}$ is omitted in the equations below.

A bushing library computes the bushing loads $\boldsymbol{\upsilon} = \begin{bmatrix} \boldsymbol{\upsilon}_{t,1} \\ \boldsymbol{\upsilon}_{r,1} \end{bmatrix}$, wherein $\boldsymbol{\upsilon}_{t,1}$ and $\boldsymbol{\upsilon}_{r,1}$ are respectively the force and torque on frame 1, resolved in frame1. These loads are function of the bushing parameters $\boldsymbol{\rho}$, the relative configuration and velocity $\mathbf{x}$ and $\mathbf{v}$ respectively. In case of refactorization of the iteration matrix of the solver, or for parameter identification purposes, the library outputs the partial derivatives of these loads as well. Following partial derivatives can be requesested: $\frac{\partial \boldsymbol{\upsilon}}{\partial \mathbf{x}}$, $\frac{\partial \boldsymbol{\upsilon}}{\partial \mathbf{v}}$, $\frac{\partial \boldsymbol{\upsilon}}{\partial \boldsymbol{\rho}}$, $\frac{\partial^2 \boldsymbol{\upsilon}}{\partial \mathbf{x} \partial \mathbf{v}}$ and $\frac{\partial^2 \boldsymbol{\upsilon}}{\partial \mathbf{v}^2}$.

---

[a] $A = \begin{bmatrix} a_{11} & a_{12} & a_{13} \\ a_{21} & a_{22} & a_{23} \\ a_{31} & a_{32} & a_{33} \end{bmatrix} \quad vect(A) = \frac{1}{2} \begin{bmatrix} a_{32} - a_{23} \\ a_{13} - a_{31} \\ a_{21} - a_{12} \end{bmatrix}$

The loads in the bushing, denoted as the loads on frame 1 and frame 2, must be in equilibrium [b]:

$$\begin{bmatrix} \boldsymbol{\upsilon}_{t,2} \\ \boldsymbol{\upsilon}_{r,2} \end{bmatrix} = - \begin{bmatrix} \mathbf{I}_3 & \mathbf{0}_3 \\ -\tilde{\mathbf{x}}_t & \mathbf{I}_3 \end{bmatrix} \begin{bmatrix} \boldsymbol{\upsilon}_{t,1} \\ \boldsymbol{\upsilon}_{r,1} \end{bmatrix} \tag{19}$$

wherein $\boldsymbol{\upsilon}_{t,2}$ and $\boldsymbol{\upsilon}_{r,2}$ are respectively the force and torque on frame 2, but resolved in frame 1.

The approach for computing the generalized force vector of a flexible joint is explained in [14]:

$$\mathrm{f}_{\mathrm{bus_i}} = \frac{\partial \mathbf{x}_t}{\partial \mathrm{q_i}}^{\mathrm{T}} \boldsymbol{\upsilon}_{t,2} + \frac{\partial \mathbf{x}_r}{\partial \mathrm{q_i}}^{\mathrm{T}} \boldsymbol{\upsilon}_{r,2} \qquad \mathrm{i} = 1, 2, \ldots, \mathrm{n_q} \tag{20}$$

with $\mathrm{f}_{\mathrm{bus_i}}$ the i-th element in the generalized bushing force vector $\mathbf{f}_{bus}$. Equation (16) requires the computation of the partial derivatives with respect to the generalized coordinates $\mathbf{q}$ and velocity $\dot{\mathbf{q}}$. These are elaborated as follows:

$$\frac{\partial \mathrm{f}_{\mathrm{bus_i}}}{\partial \mathrm{q_j}} = \frac{\partial^2 \mathbf{x}_t}{\partial \mathrm{q_j} \partial \mathrm{q_i}}^{\mathrm{T}} \boldsymbol{\upsilon}_{t,2} + \frac{\partial \mathbf{x}_t}{\partial \mathrm{q_i}}^{\mathrm{T}} \frac{\partial \boldsymbol{\upsilon}_{t,2}}{\partial \mathrm{q_j}} + \frac{\partial^2 \mathbf{x}_r}{\partial \mathrm{q_j} \partial \mathrm{q_i}}^{\mathrm{T}} \boldsymbol{\upsilon}_{r,2} + \frac{\partial \mathbf{x}_r}{\partial \mathrm{q_i}}^{\mathrm{T}} \frac{\partial \boldsymbol{\upsilon}_{r,2}}{\partial \mathrm{q_j}} \tag{21a}$$

$$\frac{\partial \mathrm{f}_{\mathrm{bus_i}}}{\partial \dot{\mathrm{q}}_\mathrm{j}} = \frac{\partial \mathbf{x}_t}{\partial \mathrm{q_i}}^{\mathrm{T}} \frac{\partial \boldsymbol{\upsilon}_{t,2}}{\partial \dot{\mathrm{q}}_\mathrm{j}} + \frac{\partial \mathbf{x}_r}{\partial \mathrm{q_i}}^{\mathrm{T}} \frac{\partial \boldsymbol{\upsilon}_{r,2}}{\partial \dot{\mathrm{q}}_\mathrm{j}} \tag{21b}$$

By applying the expressions given by Equation (19), the partial derivatives of $\boldsymbol{\upsilon}_{t,2}$ and $\boldsymbol{\upsilon}_{r,2}$ w.r.t. $\mathbf{q}$ and $\dot{\mathbf{q}}$ can be elaborated as follows :

$$\frac{\partial \boldsymbol{\upsilon}_{t,2}}{\partial \mathbf{q}} = -\frac{\partial \boldsymbol{\upsilon}_{t,1}}{\partial \mathbf{x}_t} \frac{\partial \mathbf{x}_t}{\partial \mathbf{q}} - \frac{\partial \boldsymbol{\upsilon}_{t,1}}{\partial \mathbf{v}_t} \frac{\partial \mathbf{v}_t}{\partial \mathbf{q}} \tag{22a}$$

$$\frac{\partial \boldsymbol{\upsilon}_{r,2}}{\partial \mathbf{q}} = -\left(\frac{\partial \boldsymbol{\upsilon}_{r,1}}{\partial \mathbf{x}_r} \frac{\partial \mathbf{x}_r}{\partial \mathbf{q}} + \frac{\partial \boldsymbol{\upsilon}_{r,1}}{\partial \boldsymbol{\omega}_r} \frac{\partial \boldsymbol{\omega}_r}{\partial \mathbf{q}} \right) + \frac{\partial \tilde{\mathbf{x}}_t}{\partial \mathbf{q}} \boldsymbol{\upsilon}_{t,1} + \tilde{\mathbf{x}}_t \left(\frac{\partial \boldsymbol{\upsilon}_{t,1}}{\partial \mathbf{x}_t} \frac{\partial \mathbf{x}_t}{\partial \mathbf{q}} + \frac{\partial \boldsymbol{\upsilon}_{t,1}}{\partial \mathbf{v}_t} \frac{\partial \mathbf{v}_t}{\partial \mathbf{q}} \right) \tag{22b}$$

$$\frac{\partial \boldsymbol{\upsilon}_{t,2}}{\partial \dot{\mathbf{q}}} = -\frac{\partial \boldsymbol{\upsilon}_{t,1}}{\partial \mathbf{v}_t} \frac{\partial \mathbf{v}_t}{\partial \dot{\mathbf{q}}} \tag{22c}$$

$$\frac{\partial \boldsymbol{\upsilon}_{r,2}}{\partial \dot{\mathbf{q}}} = -\frac{\partial \boldsymbol{\upsilon}_{r,1}}{\partial \boldsymbol{\omega}_r} \frac{\partial \boldsymbol{\omega}_r}{\partial \dot{\mathbf{q}}} + \tilde{\mathbf{x}}_t \frac{\partial \boldsymbol{\upsilon}_{t,1}}{\partial \mathbf{v}_t} \frac{\partial \mathbf{v}_t}{\partial \dot{\mathbf{q}}} \tag{22d}$$

wherein the first and second order partial derivatives of the relative configuration $\mathbf{x}$ with respect to the generalized coordinates $\mathbf{q}$ are given by:

$$\frac{\partial \mathbf{x}_t}{\partial \mathrm{q_i}}^{\mathrm{T}} = \left(\mathbf{u}_2^{\mathrm{T}} - \mathbf{u}_1^{\mathrm{T}} \right) \frac{\partial \mathbf{R}_1}{\partial \mathrm{q_i}} + \left(\frac{\partial \mathbf{u}_2}{\partial \mathrm{q_i}}^{\mathrm{T}} - \frac{\partial \mathbf{u}_1}{\partial \mathrm{q_i}}^{\mathrm{T}} \right) \mathbf{R}_1 \tag{23a}$$

$$\frac{\partial^2 \mathbf{x}_t}{\partial \mathrm{q_j} \partial \mathrm{q_i}}^{\mathrm{T}} = \left(\frac{\partial \mathbf{u}_2}{\partial \mathrm{q_j}}^{\mathrm{T}} - \frac{\partial \mathbf{u}_1}{\partial \mathrm{q_j}}^{\mathrm{T}} \right) \frac{\partial \mathbf{R}_1}{\partial \mathrm{q_i}} + \left(\frac{\partial \mathbf{u}_2}{\partial \mathrm{q_i}}^{\mathrm{T}} - \frac{\partial \mathbf{u}_1}{\partial \mathrm{q_i}}^{\mathrm{T}} \right) \frac{\partial \mathbf{R}_1}{\partial \mathrm{q_j}} \tag{23b}$$

$$\frac{\partial \mathbf{x}_r}{\partial \mathrm{q_i}}^{\mathrm{T}} = vect \left(\frac{\partial \mathbf{R}_1}{\partial \mathrm{q_i}}^{\mathrm{T}} \mathbf{R}_1 + \mathbf{R}_1^{\mathrm{T}} \left(\frac{\partial \mathbf{R}_2}{\partial \mathrm{q_i}} \mathbf{R}_2^{\mathrm{T}} \right) \mathbf{R}_1 \right)^{\mathrm{T}} \tag{23c}$$

$$\begin{aligned} \frac{\partial^2 \mathbf{x}_r}{\partial \mathrm{q_j} \partial \mathrm{q_i}}^{\mathrm{T}} = vect \Bigg(& \frac{\partial \mathbf{R}_1}{\partial \mathrm{q_i}}^{\mathrm{T}} \frac{\partial \mathbf{R}_1}{\partial \mathrm{q_j}} + \frac{\partial \mathbf{R}_1}{\partial \mathrm{q_j}}^{\mathrm{T}} \left(\frac{\partial \mathbf{R}_2}{\partial \mathrm{q_i}} \mathbf{R}_2^{\mathrm{T}} \right) \mathbf{R}_1 + \\ & \mathbf{R}_1^{\mathrm{T}} \left(\frac{\partial \mathbf{R}_2}{\partial \mathrm{q_i}} \mathbf{R}_2^{\mathrm{T}} \right) \frac{\partial \mathbf{R}_1}{\partial \mathrm{q_j}} + \mathbf{R}_1^{\mathrm{T}} \left(\frac{\partial \mathbf{R}_2}{\partial \mathrm{q_i}} \frac{\partial \mathbf{R}_2}{\partial \mathrm{q_j}}^{\mathrm{T}} \right) \mathbf{R}_1 \Bigg)^{\mathrm{T}} \end{aligned} \tag{23d}$$

---

[b] $v = \begin{bmatrix} v_1 \\ v_2 \\ v_3 \end{bmatrix} \quad \tilde{v} = \begin{bmatrix} 0 & -v_3 & v_2 \\ v_3 & 0 & -v_1 \\ -v_2 & v_1 & 0 \end{bmatrix}$

the first and second order partial derivative of the relative velocity $\mathbf{v}$ w.r.t. $\mathbf{q}$ and $\dot{\mathbf{q}}$ is given by:

$$\frac{\partial \mathbf{v}_t}{\partial \mathrm{q_i}}^{\mathrm{T}} = \left(\dot{\mathbf{u}}_2^{\mathrm{T}} - \dot{\mathbf{u}}_1^{\mathrm{T}}\right) \frac{\partial \mathbf{R}_1}{\partial \mathrm{q_i}} \tag{24a}$$

$$\frac{\partial \mathbf{v}_t}{\partial \dot{\mathrm{q}}_\mathrm{i}}^{\mathrm{T}} = \left(\frac{\partial \mathbf{u}_2}{\partial \mathrm{q_i}}^{\mathrm{T}} - \frac{\partial \mathbf{u}_1}{\partial \mathrm{q_i}}^{\mathrm{T}}\right) \mathrm{R}_1 \tag{24b}$$

$$\frac{\partial \boldsymbol{\omega}_r}{\partial \mathrm{q_i}}^{\mathrm{T}} = \left(vect\left(\frac{\mathrm{d}\mathbf{R}_2}{\mathrm{dt}} \frac{\partial \mathbf{R}_2}{\partial \mathrm{q_i}}^{\mathrm{T}}\right) - vect\left(\frac{\mathrm{d}\mathbf{R}_1}{\mathrm{dt}} \frac{\partial \mathbf{R}_1}{\partial \mathrm{q_i}}^{\mathrm{T}}\right)\right)^{\mathrm{T}} \mathrm{R}_1 + \left(\boldsymbol{\omega}_2 - \boldsymbol{\omega}_1\right)^{\mathrm{T}} \frac{\partial \mathbf{R}_1}{\partial \mathrm{q_i}} \tag{24c}$$

$$\frac{\partial \boldsymbol{\omega}_r}{\partial \dot{\mathrm{q}}_\mathrm{i}}^{\mathrm{T}} = \left(vect\left(\frac{\partial \mathbf{R}_2}{\partial \mathrm{q_i}} \mathbf{R}_2^{\mathrm{T}}\right) - vect\left(\frac{\partial \mathbf{R}_1}{\partial \mathrm{q_i}} \mathbf{R}_1^{\mathrm{T}}\right)\right)^{\mathrm{T}} \mathrm{R}_1 \tag{24d}$$

The computation of Equation (16c), with $\frac{\partial \mathbf{f}_{ext}}{\partial \dot{\mathbf{q}}}$ being zero, is elaborated as follows:

$$\frac{\mathrm{d}}{\mathrm{dt}}\left(\frac{\partial \mathrm{f}_{\mathrm{bus_i}}}{\partial \dot{\mathrm{q}}_\mathrm{j}}\right) = \frac{\mathrm{d}}{\mathrm{dt}}\left(\frac{\partial \mathbf{x}_t}{\partial \mathrm{q_i}}^{\mathrm{T}}\right) \frac{\partial \boldsymbol{\upsilon}_{t,2}}{\partial \dot{\mathrm{q}}_\mathrm{j}} + \frac{\partial \mathbf{x}_t}{\partial \mathrm{q_i}}^{\mathrm{T}} \frac{\mathrm{d}}{\mathrm{dt}}\left(\frac{\partial \boldsymbol{\upsilon}_{t,2}}{\partial \dot{\mathrm{q}}_\mathrm{j}}\right) + \frac{\mathrm{d}}{\mathrm{dt}}\left(\frac{\partial \mathbf{x}_r}{\partial \mathrm{q_i}}^{\mathrm{T}}\right) \frac{\partial \boldsymbol{\upsilon}_{r,2}}{\partial \dot{\mathrm{q}}_\mathrm{j}} + \frac{\partial \mathbf{x}_r}{\partial \mathrm{q_i}}^{\mathrm{T}} \frac{\mathrm{d}}{\mathrm{dt}}\left(\frac{\partial \boldsymbol{\upsilon}_{r,2}}{\partial \dot{\mathrm{q}}_\mathrm{j}}\right) \tag{25}$$

where the time derivatives of the factors are given by:

$$\frac{\mathrm{d}}{\mathrm{dt}}\left(\frac{\partial \boldsymbol{\upsilon}_{t,2}}{\partial \dot{\mathbf{q}}}\right) = \frac{\mathrm{d}}{\mathrm{dt}}\left(-\frac{\partial \boldsymbol{\upsilon}_{t,1}}{\partial \mathbf{v}_t}\right) \frac{\partial \mathbf{v}_t}{\partial \dot{\mathbf{q}}} - \frac{\partial \boldsymbol{\upsilon}_{t,1}}{\partial \mathbf{v}_t} \frac{\mathrm{d}}{\mathrm{dt}}\left(\frac{\partial \mathbf{v}_t}{\partial \dot{\mathbf{q}}}\right) \tag{26a}$$

$$\begin{aligned}\frac{\mathrm{d}}{\mathrm{dt}}\left(\frac{\partial \boldsymbol{\upsilon}_{r,2}}{\partial \dot{\mathbf{q}}}\right) = {} & \frac{\mathrm{d}}{\mathrm{dt}}\left(-\frac{\partial \boldsymbol{\upsilon}_{r,1}}{\partial \boldsymbol{\omega}_r}\right) \frac{\partial \boldsymbol{\omega}_r}{\partial \dot{\mathbf{q}}} - \frac{\partial \boldsymbol{\upsilon}_{r,1}}{\partial \boldsymbol{\omega}_r} \frac{\mathrm{d}}{\mathrm{dt}}\left(\frac{\partial \boldsymbol{\omega}_r}{\partial \dot{\mathbf{q}}}\right) + \dot{\tilde{\mathbf{x}}}_t \frac{\partial \boldsymbol{\upsilon}_{t,1}}{\partial \mathbf{v}_t} \frac{\partial \mathbf{v}_t}{\partial \dot{\mathbf{q}}} + \\ & \tilde{\mathbf{x}}_t \frac{\mathrm{d}}{\mathrm{dt}}\left(\frac{\partial \boldsymbol{\upsilon}_{t,1}}{\partial \mathbf{v}_t}\right) \frac{\partial \mathbf{v}_t}{\partial \dot{\mathbf{q}}} + \tilde{\mathbf{x}}_t \frac{\partial \boldsymbol{\upsilon}_{t,1}}{\partial \mathbf{v}_t} \frac{\mathrm{d}}{\mathrm{dt}}\left(\frac{\partial \mathbf{v}_t}{\partial \dot{\mathbf{q}}}\right)\end{aligned} \tag{26b}$$

$$\frac{\mathrm{d}}{\mathrm{dt}}\left(\frac{\partial \boldsymbol{\upsilon}}{\partial \mathbf{v}}\right) = \frac{\partial^2 \boldsymbol{\upsilon}}{\partial \mathbf{x} \partial \mathbf{v}} \mathbf{v} + \frac{\partial^2 \boldsymbol{\upsilon}}{\partial \mathbf{v}^2} \mathbf{a} \tag{26c}$$

$$\frac{\mathrm{d}}{\mathrm{dt}}\left(\frac{\partial \mathbf{v}_t}{\partial \dot{\mathrm{q}}_\mathrm{i}}^{\mathrm{T}}\right) = \mathbf{0} \tag{26d}$$

$$\frac{\mathrm{d}}{\mathrm{dt}}\left(\frac{\partial \boldsymbol{\omega}_r}{\partial \dot{\mathrm{q}}_\mathrm{i}}^{\mathrm{T}}\right) = \left(vect\left(\frac{\partial \mathbf{R}_2}{\partial \mathrm{q_i}} \frac{\mathrm{d}\mathbf{R}_2^{\mathrm{T}}}{\mathrm{dt}}\right) - vect\left(\frac{\partial \mathbf{R}_1}{\partial \mathrm{q_i}} \frac{\mathrm{d}\mathbf{R}_1^{\mathrm{T}}}{\mathrm{dt}}\right)\right)^{\mathrm{T}} \mathrm{R}_1 \tag{26e}$$

wherein the time derivative of the rotation matrices is given by

$$\frac{\mathrm{d}\mathbf{R}_\mathrm{i}}{\mathrm{dt}} = \sum_n \frac{\partial \mathbf{R}_\mathrm{i}}{\partial \mathrm{q_n}} \dot{\mathrm{q}}_\mathrm{n} \qquad \mathrm{i} = 1,2 \tag{27}$$

$$\tag{28}$$

and the relative acceleration vector $\mathbf{a} = \begin{bmatrix} \mathbf{a}_t \\ \boldsymbol{\alpha}_r \end{bmatrix}$ is given by

$$\mathbf{a}_t = \mathbf{R}_1^{\mathrm{T}} \left(\ddot{\mathbf{u}}_2^{(p)} - \ddot{\mathbf{u}}_1^{(p)}\right) \tag{29a}$$

$$\boldsymbol{\alpha}_r = \mathbf{R}_1^{\mathrm{T}} \left(\dot{\boldsymbol{\omega}}_2^{(p)} - \dot{\boldsymbol{\omega}}_1^{(p)}\right) \tag{29b}$$

wherein $\dot{\boldsymbol{\omega}}_1$ and $\dot{\boldsymbol{\omega}}_2$ are respectively the angular accelerations of frame 1 and 2, resolved in the fixed world coordinate system.

4.2.2 Effect of FNCF on generalized bushing force

Because of the use of the FNCF formulation, it can be observed in section 4.2.1 that the computation of the partial derivatives are significantly reduced in complexity with respect to the general case as presented by Zhu [13] . Several terms are completely eliminated, i.e:

$$\frac{\mathrm{d}}{\mathrm{dt}}\left(\frac{\partial \mathbf{R}}{\partial \mathrm{q_i}}\right) = \sum_n \frac{\partial^2 \mathbf{R}}{\partial \mathrm{q_i} \partial \mathrm{q_n}} \dot{\mathrm{q}}_\mathrm{n} = 0 \tag{30a}$$

$$\frac{\partial^2 \mathbf{R}}{\partial \mathrm{q_j} \partial \mathrm{q_i}} = 0 \tag{30b}$$

$$\frac{\partial^2 \mathbf{u}}{\partial \mathrm{q_j} \partial \mathrm{q_i}} = 0 \tag{30c}$$

$$\frac{\partial \dot{\mathbf{u}}}{\partial \mathrm{q_i}} = 0 \tag{30d}$$

Moreover, several remaining terms are constant:

$$\frac{\partial \mathbf{R}}{\partial \mathrm{q_i}} = cte_1 \tag{31a}$$

$$\frac{\partial \mathbf{u}}{\partial \mathrm{q_i}} = cte_2 \tag{31b}$$

4.2.3 Least squares error of the optimization signal and its derivatives

The least squares error function g is given in Equation (1b). In this work it is assumed that the simulated signal y and the measured signal $\hat{y}$, are position signals. In general other signals such as velocities, accelerations, forces, etc... can be employed. This results in g being denoted as:

$$g = \left(u_i^{(p)} - \hat{x}(t)\right)^2 \tag{32}$$

wherein $u_i^{(p)}$ as described in Equation (4) and $\hat{x}(t)$ being the measured position signal. The partial derivatives of g are elaborated as follows:

$$g_\mathbf{q} = 2\left(u_i^{(p)} - \hat{u}_i^{(p)}\right)\frac{\partial u_i^{(p)}}{\partial \mathbf{q}} = 2\left(u_i^{(p)} - \hat{u}_i^{(p)}\right) r_{i\mathbf{q}}^{(p)} \tag{33a}$$

$$g_{\dot{\mathbf{q}}} = g_{\ddot{\mathbf{q}}} = g_{\boldsymbol{\rho}} = \mathbf{0} \tag{33b}$$

5 Numerical validation

The proposed bushing identification approach is numerically demonstrated on an academic double mass-spring-damper system, shown in Fig. 2, which is implemented in a general multibody framework. The bushings are modeled by the Kelvin-Voigt model, represented by a spring and damper in parallel. In this example the position signal x_2 will be used for the identification of the bushing parameters. The input to the system is a force applied on mass m_1. The reference response is generated from a simulation with the correct stiffness and damping parameters. The initial guesses $\boldsymbol{\rho}_{init}$ for the parameters to identify are the exact values divided by a factor two. The convergence of the identified response to the reference for the different iterations, is shown in Fig. 3. This figure shows that the propose method rapidly drives the parameters to a configuration where the measured and simulated responses correspond well.

The accompanying identified parameter values per iteration are shown in Figs. 4– 5. This figure also shows rapid convergence to the correct parameter values for the stiffness and damping of the unknown bushings. This academic example demonstrates the accurate operation of the proposed approach.

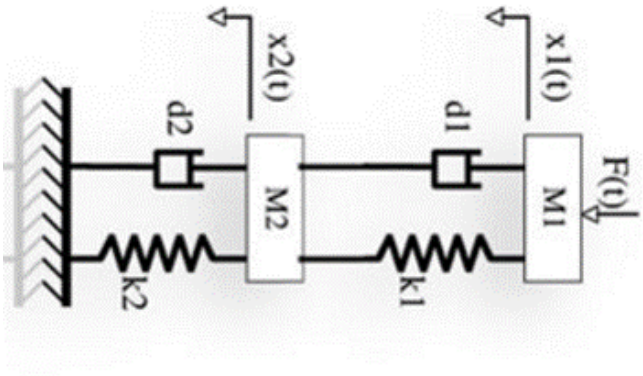

Fig. 2: Double mass-spring-damper system

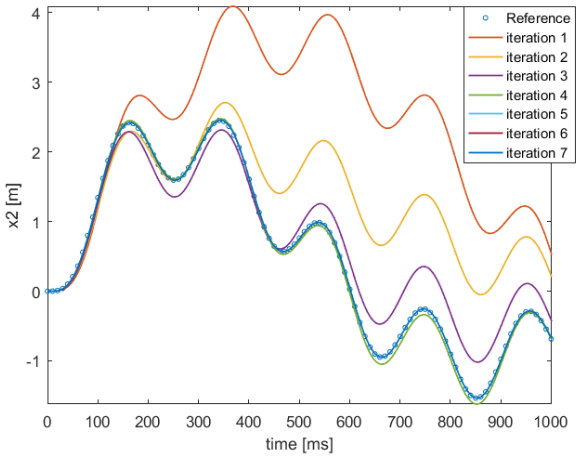

Fig. 3: Response per iteration

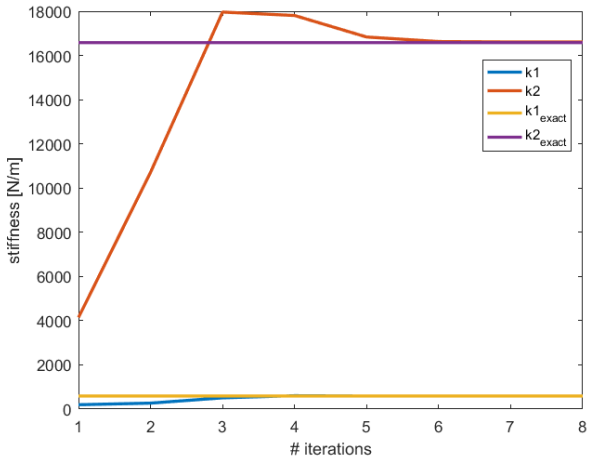

Fig. 4: Stiffness parameters per iteration

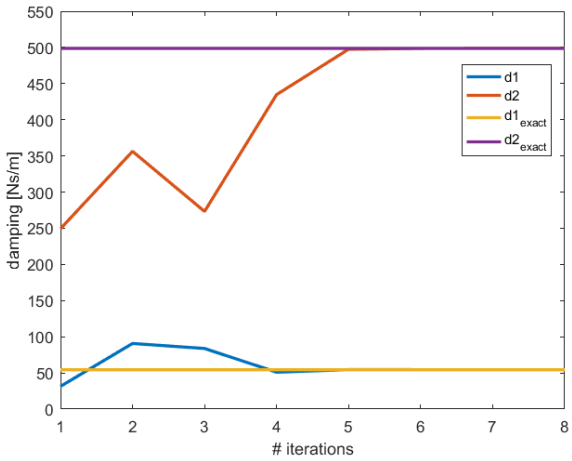

Fig. 5: Damping parameters per iteration

6 Conclusions

This work proposes a technique for identifying bushing parameters in-situ using system-level measurements and (flexible) multibody models. The sensitivity information is obtained using the adjoint variable method (AVM) in combination with the recently developed flexible natural coordinate formulation (FNCF) multibody methodology. The proposed approach of combining the AVM approach with the FNCF model results in a significant decrease in the computational cost with respect to alternative approaches based on other sensitivity approache and other multibody formulations. This is due to the good scaling of the AVM with respect to an increasing number of parameters and the simple structure of the FNCF model. The appraoch moreover leads to a limited implementation cost, as the equations of motion ant their partial derivatives can be readily obtained and are of limited order for the FNCF formulation. The proposed methodology is demonstrated on an academic example for a double mass-spring-damped implemented in a general multibody code. Future work will focus on performing studies on larger scale problems with many different components and strongly nonlinear bushing characteristics.

Acknowledgements

The research of S. Vanpaemel and F. Naets is funded by a grant from the Research Foundation – Flanders (FWO). Furthermore the Research Fund KU Leuven and the Flanders Innovation & Entrepreneurship Agency within the WeReClean project, are gratefully acknowledged for their support.

References

[1] S. Dzierzek, "Experiment-based modeling of cylindrical rubber bushings for the simulation of wheel suspension dynamic behavior," SAE Technical Paper, 2000.

[2] M. Berg, "A Non-Linear Rubber Spring Model for Rail Vehicle Dynamics Analysis," *Vehicle System Dynamics*, vol. 30, pp. 197–212, Sept. 1998.

[3] K. Sedlaczek, S. Dronka, and J. Rauh, "Advanced modular modelling of rubber bushings for vehicle simulations," *Vehicle System Dynamics*, vol. 49, pp. 741–759, May 2011.

[4] J. Nocedal and S. J. Wright, *Numerical optimization*. Springer series in operations research, New York: Springer, 2nd ed ed., 2006. OCLC: ocm68629100.

[5] R. Serban and J. S. Freeman, "Identification and Identifiability of Unknown Parameters in Multibody Dynamic Systems," *Multibody System Dynamics*, vol. 5, pp. 335–350, May 2001.

[6] E. J. Haug, "Design Sensitivity Analysis of Dynamic Systems," in *Computer Aided Optimal Design: Structural and Mechanical Systems*, NATO ASI Series, pp. 705–755, Springer, Berlin, Heidelberg, 1987.

[7] D. Bestle and P. Eberhard, "Analyzing and Optimizing Multibody Systems," *Mechanics of Structures and Machines*, vol. 20, pp. 67–92, Jan. 1992.

[8] C. H. Bischof, "On the Automatic Differentiation of Computer Programs and an Application to Multibody Systems," in *IUTAM Symposium on Optimization of Mechanical Systems*, Solid Mechanics and its Applications, pp. 41–48, Springer, Dordrecht, 1996.

[9] O. Brüls and P. Eberhard, "Sensitivity analysis for dynamic mechanical systems with finite rotations," *International Journal for Numerical Methods in Engineering*, vol. 74, pp. 1897–1927, June 2008.

[10] J. Banerjee, "Graph-theoretic sensitivity analysis of dynamic systems," 2013.

[11] J. R. Martins, "A coupled-adjoint method for high-fidelity aero-structural optimization," tech. rep., STANFORD UNIV CA DEPT OF AERONAUTICS AND ASTRONAUTICS, 2002.

[12] M. Vermaut, F. Naets, and W. Desmet, "A flexible natural coordinates formulation (fncf) for the efficient simulation of small-deformation multibody systems," *Int. J. of Numerical Methods in Engineering*, 2018 (accepted).

[13] Y. Zhu, "Sensitivity Analysis and Optimization of Multibody Systems," 2014.

[14] O. A. Bauchau, *Flexible Multibody Dynamics*, vol. 176 of *Solid Mechanics and Its Applications*. Dordrecht: Springer Netherlands, 2011.